# ELOVL1 production of C24 acyl-CoAs is linked to C24 sphingolipid synthesis

**Yusuke Ohno[a,1], Shota Suto[a,1], Masao Yamanaka[a], Yukiko Mizutani[b], Susumu Mitsutake[b], Yasuyuki Igarashi[b], Takayuki Sassa[a], and Akio Kihara[a,2]**

[a]Laboratory of Biochemistry, Faculty of Pharmaceutical Sciences, Hokkaido University, Kita 12-jo, Nishi 6-chome, Kita-ku, Sapporo 060-0812, Japan

[b]Laboratory of Biomembrane and Biofunctional Chemistry, Faculty of Advanced Life Sciences, Hokkaido University, Kita 21-jo, Nishi 11-choume, Kita-ku, Sapporo 001-0021, Japan

[1]Y.O. and S.S. contributed equally to this manuscript

[2]To whom correspondence should be addressed:

Akio Kihara

Laboratory of Biochemistry, Faculty of Pharmaceutical Sciences, Hokkaido University

Kita 12-jo, Nishi 6-choume, Kita-ku, Sapporo 060-0812, Japan

Tel: +81-11-706-3754

Fax: +81-11-706-4900

E-mail: kihara@pharm.hokudai.ac.jp

## Abstract

Very long-chain fatty acids (VLCFAs) exert a variety of cellular functions and are associated with numerous diseases. However, the precise pathway behind their elongation has remained elusive. Moreover, few regulatory mechanisms for VLCFAs synthesis have been identified. Elongases catalyze the first of four steps in the VLCFA elongation cycle; mammals have seven elongases (ELOVL1-7). In the present study, we determined the precise substrate specificities of all the ELOVLs by *in vitro* analyses. Particularly notable was the high activity exhibited by ELOVL1 toward saturated and monounsaturated C20- and C22-CoAs, and that it was essential for the production of C24 sphingolipids, which are unique in their capacity to interdigitate within the membrane as a result of their long chain length. We further established that ELOVL1 activity is regulated with the ceramide synthase CERS2, an enzyme essential for C24 sphingolipid synthesis. This regulation may ensure that the production of C24-CoA by elongation is coordinated with its utilization. Finally, knock-down of *ELOVL1* caused a reduction in the activity of the Src kinase LYN, confirming that C24-sphingolipids are particularly important in membrane microdomain function.

Keywords: elongase/fatty acid/lipid/sphingolipid/very long-chain fatty acid

## Introduction

Lipid metabolism is closely related to metabolic syndrome and lifestyle-related diseases including hyperlipidemia, obesity, and arteriosclerosis. Fatty acid (FA) species found in cells and in plasma lipids, such as triglycerides and cholesterol esters, are mainly C16 (C16:0, palmitic acid) and C18 (C18:1, oleic acid; C18:2, linoleic acid) long-chain FAs (LCFAs) (1). Less common FAs having longer chain length and/or a higher degree of unsaturation exhibit completely different, often beneficial, physiological and pathological properties from those of LCFAs. FAs with a chain length of≥20 are called very long -chain FAs (VLCFAs). VLCFAs are characteristically divided into saturated, monounsaturated, n-6 polyunsaturated, and n-3 polyunsaturated FAs (PUFAs), each of which exhibit distinct functions and properties. Most saturated and monounsaturated VLCFAs are sphingolipid components and so play important roles in skin barrier formation and neural functions (2, 3). n-6 PUFAs (*e.g.* C20:4) are involved in the promotion of inflammation as precursors of eicosanoids (4). n-3 PUFAs (*e.g.* C20:5 and C22:6) are effective in the prevention of arteriosclerosis, heart failure, and age-related macular degeneration by virtue of their roles in reducing plasma triglycerides, lowering blood pressure, and suppressing inflammation (5).

Sphingolipids are major lipid components of eukaryotic plasma membranes, along with glycerophospholipids and cholesterol. Ceramide (Cer), the sphingolipid backbone, comprises a long-chain base attached to FA via an amide bond. In mammalian tissues, C16:0 FA and C24 (C24:0 and C24:1) VLCFAs are the most common FAs. Sphingolipids characteristically carry a C24 FA. This long C24 moiety would be expected to interdigitate within the plasma membrane. Indeed, in one study, C24 lactosylceramide in the outer leaflet of the plasma membrane interacted with the Src family kinase LYN, which is expressed and functions in leukocytes, anchored to the inner leaflet (6).

VLCFAs are produced from certain LCFAs, provided through diet or generated by FA

synthase, or they are elongated from shorter VLCFAs by endoplasmic reticulum (ER) membrane-bound enzymes, which lengthen each chain with carbon units from FAs that have been converted to substrate-form acyl-CoAs (7). The FA elongase machinery comprises four distinct enzymes. The first type, known as elongases, condenses acyl-CoA and malonyl-CoA to produce 3-ketoacyl-CoA; this step is rate-limiting in VLCFA synthesis. To date, seven elongases (ELOVL1-7) have been identified in mammals and characterized (8, 9) [supporting information (SI) Table S1]. The elongases ELOVL1-7 have each been shown to exhibit characteristic substrate specificities (8, 9) (Table S1), yet their precise roles in the VLCFA elongation pathways have not been completely determined. This dearth of information is due to insufficient or incomplete biochemical analyses, limited substrates, and inconsistent techniques among researchers (Table S1).

In addition to better understanding the roles the ELOVLs and their substrate specificities in VLCFA elongation, it is necessary to also recognize the role of regulation in these pathways, as well as the interaction with other lipid systems. Cer synthases catalyze the synthesis of Cer from long-chain base and fatty acyl-CoA. Each of 6 mammalian Cer synthases (CERS1-6) exhibits its own characteristic substrate specificity toward certain fatty acyl-CoA(s) (2). Recent studies using *CerS2* knockout mice revealed that CerS2 is the predominant Cer synthase for C24 Cer production (3, 13). These mice exhibited severe hepatopathy, myelin sheath defects, and cerebellar degeneration (3, 14).

In the presented studies, we have analyzed *in vitro*, detailed substrate specificities of all the ELOVLs and provide an overall summary of the VLCFA synthetic pathways. Especially significant is the demonstrated importance of ELOVL1 in the production of C24-CoA, the substrate of C24 sphingolipids. Of even more notable interest, we found a regulation of ELOVL1 by CERS2 and established a close link between VLCFA elongation and C24 Cer production.

## Results

### Determination of substrate specificities of ELOVL proteins

Although ELOVL1 has been predicted to be involved in the production of C24 sphingolipids based on studies using elongase-null yeast mutants expressing ELOVL1 (10, 11), its precise substrate specificities toward acyl-CoAs have not been determined by direct, biochemical analysis. Moreover, the substrates for other ELOVLs have also not been precisely determined due to insufficient or incomplete biochemical analyses, limited substrates, and inconsistent techniques among researchers (Table S1). Therefore, we first determined the substrate specificity of each ELOVL protein under standardized conditions. For this purpose, we cloned the *ELOVL* genes and expressed them in HEK 293T cells as N-terminally triple FLAG (3xFLAG)-tagged proteins. By immunoblotting with an anti-FLAG antibody, ELOVL1, 2, 5, and 7 were each detected as a single band, however two bands were observed for ELOVL3, 4, and 6 (Fig. S1*A*). The upper bands represent their *N*-glycosylated forms, since these shifted to low molecular weight bands upon treatment with endoglycosidase H (Endo H) (Fig. S1*B*), which removes high mannose-type glycosylation. Indirect immunofluorescence microscopy revealed that all ELOVLs were localized in the ER (Fig. S2). This localization is reasonable, since VLCFA synthesis occurs there.

We performed *in vitro* elongase assays using total membrane fractions prepared from HEK 293T cells overproducing each ELOVL, and a mixture containing [$^{14}$C]malonyl-CoA and one of 11 different acyl-CoAs (C16:0-, C18:0-, C18:1(n-9)-, C18:2(n-6)-, C18:3(n-3)-, C18:3(n-6)-, C20:0-, C20:4(n-6)-, C22:0-, C24:0-, or C26:0-CoA). The ELOVL protein levels in the membrane fractions were determined to be expressed at similar levels by immunoblotting following treatment with Endo H (Fig. 1*A*). ELOVL1 elongated saturated C18:0-C26:0 acyl-CoAs, with the highest activity toward C22:0-CoA, yet had no elongation activity toward unsaturated acyl-CoA (Fig. 1*B*). Of the ELOVLs, ELOVL1 was the most

potent elongase for C22:0-, C24:0-, and C26:0-CoAs. ELOVL3 and 7 also elongated C18:0-CoA, and generally exhibited similar substrate specificities (Fig. 1*B*). Their highest activities were toward C18-CoAs (especially C18:0-CoA for ELOVL3 and C18:3(n-3)-CoA for ELOVL7), relatively independently of the number of double bonds. Both also exhibited activities toward C16-C22 acyl-CoAs. ELOVL4 elongated C24:0- and C26:0-CoAs with weak but significant activities (Fig. 1*B*). The activity of ELOVL6 was extremely high toward C16:0-CoA (Fig. 1*B*). As reported previously (15-18), ELOVL2 and 5 acted specifically toward polyunsaturated acyl-CoAs, and were the most potent elongases for C20:4(n-6)-CoA and C18:3(n-6)-CoAs, respectively (Fig. 1*B*).

In the above assays, the product FAs were separated by normal-phase TLC, which does not efficiently separate FAs with different chain lengths. Therefore, it remained unclear how many elongation cycles occurred in each reaction. For example, since ELOVL1 could elongate C18:0-C26:0 acyl-CoAs, we postulated that ELOVL1 elongated C18:0-CoA not only to C20:0-CoA but also further to form the longer acyl-CoAs. To test this possibility, we separated the product FAs of the elongase assays by reverse-phase TLC. We indeed found that substantial amounts of C24:0- and C26:0-CoA were produced by ELOVL1 when C18:0-CoA was used as a substrate (Fig. 1*C*). In contrast, ELOVL3 and 7 elongated C18:0-CoA mainly to C20:0-CoA, although low levels of C22:0-CoA were observed (Fig. 1*C*). Similarly, ELOVL1 but not ELOVL3 elongated C20:0-CoA efficiently to C24:0-CoA (Fig. 1*C*).

In the yeast *Saccharomyces cerevisiae*, VLCFAs are almost exclusively C26:0 FAs with or without α-hydroxylation, and no PUFAs exist. Yeast have 3 elongases, Elo1, Fen1 (Elo2), and Sur4 (Elo3). Fen1 and Sur4 elongate long-chain acyl-CoAs to C22:0-CoA (weakly to C24:0-CoA) and C26:0-CoA, respectively (19, 20). Since VLCFA production is essential for yeast growth, double deletion of *FEN1* and *SUR4* genes is lethal (10, 21). Reportedly, *ELOVL1* can rescue the lethality of Δ*fen1* Δ*sur4* cells (22). We confirmed this, and

additionally found that *ELOVL3* and *ELOVL7* can restore the growth defects of conditional Δ*fen1* Δ*sur4* cells, although weakly, especially for *ELOVL3* (Fig. S3*A*); findings are detailed in the SI text. Using GC/MS, we further confirmed the production of C24:0-CoAs in cells expressing ELOVL1 (Fig. S3*C*). In summary, ELOVL1, 3, and 7 exhibit activities for elongating saturated long-chain acyl-CoAs to very long-chain acyl-CoAs.

**Tissue-specific distribution of ELOVLs**

To investigate the tissue-specific expression pattern of each *ELOVL* mRNA, we performed RT-PCR analyses using human cDNAs of 16 different tissues (Fig. 2). *ELOVL1*, *ELOVL5*, and *ELOVL6* mRNAs were expressed ubiquitously. *ELOVL4* mRNA was expressed in many tissues, but its expression levels varied, being highest in thymus, followed by testis, small intestine, ovary, and prostate. Little or no *ELOVL4* was expressed in heart, lung, liver, or leukocytes. The *ELOVL7* mRNA was also expressed in most tissues tested except heart and skeletal muscle. Expression in pancreas, kidney, prostate, and colon was high, whereas that in lung, ovary, spleen, and thymus was low. Two bands were produced by *ELOVL7*-specific primers. Sequencing analyses revealed that the upper band was a splicing isoform and contained an additional 119 bp nucleotides between 65G and 66A of the *ELOVL7* coding region. This sequence contained a stop codon, resulting in the production of a protein with very low molecular mass (3 kDa). The role of this splicing isoform is unclear, but it may be functionless. *ELOVL2* and *ELOVL3* mRNA expression was highly tissue-specific. High expression of *ELOVL2* was observed only in liver and testis, with weak expression in pancreas, placenta, and prostate. Significant expression of *ELOVL3* was detected only in testis. These results indicate that each ELOVL exhibits a characteristic tissue-expression pattern, although expression levels of certain ELOVLs may be changed in certain tissues under different conditions.

**ELOVL1 is important for C24 Cer synthesis**

The *in vitro* results (Fig. 1*B* and *C*) and yeast complementation analyses (Fig. S3) (22) suggest that ELOVL1 is important for C24 sphingolipid synthesis, yet this possibility has not been proven using mammalian cells. To confirm this, we performed knock-down analysis using HeLa cells and siRNA specific to *ELOVL1*. Total membrane fractions prepared from HeLa cells treated with *ELOVL1* siRNA exhibited significantly lower activities toward C18:0-, C20:0-, and C22:0-CoAs, but not toward C16:0- or C18:3(n-3)-CoA compared to control cells (Fig. 3*A*), agreeing the *in vitro* results (Fig. 1*B*). Efficiency of the knock-down of mRNA levels by the *ELOVL1* siRNA was confirmed by RT-PCR analysis (Fig. 3*B*). In HeLa cells, neither *ELOVL2* nor *ELOVL4* is expressed, and the mRNA levels of the other expressed *ELOVLs* were not affected by the *ELOVL1* siRNA (Fig. S4). We also confirmed that in the human *ELOVL1* siRNA-treated HeLa cells, expression of mouse Elovl1 reversed the inhibitory effects on the elongase activities toward C20:0- and C22:0-CoAs (Fig. S5).

To examine the effect of the *ELOVL1* siRNA on the chain length of Cer, we next performed [$^3$H]sphingosine labeling experiments. HeLa cells treated with control siRNA or *ELOVL1* siRNA were labeled with [$^3$H]sphingosine, then lipids were extracted and separated by reverse-phase TLC. Control cells produced high levels of C24:1 Cer and, to a lesser extent, C24:0 Cer, whereas treatment with the *ELOVL1* siRNA resulted in a reduction in these C24 Cers and an increase in C16:0 and C18:0 Cers (Fig. 3*C*). Liquid chromatography (LC)/MS analysis measuring sphingomyelins (SMs) revealed that C24 SMs were abundant in the HeLa cells treated with the control siRNA, but were reduced in those treated with the *ELOVL1* siRNA; instead, C16:0 and C18:0 SMs were increased (Fig. 3*D*).

The above analyses indicate that ELOVL1 is important not only for C24:0 production but also for production of C24:1 sphigolipids. However, in the above *in vitro* analysis (Fig. 1*B*),

we were not able to test the ELOVL1 activity toward C20:1(n-9)- or C22:1(n-9)-CoAs due to the unavailability of these acyl-CoAs. Therefore, we performed an *in vitro* elongase assay using FAs, CoA, and ATP instead of acyl-CoAs. We found that ELOVL1 also exhibits activity toward C20:1(n-9) and C22:1(n-9) FAs, similar to that observed toward the positive control C20:0 FA (Fig. S6). These results demonstrate that ELOVL1 is important in the synthesis of both saturated and monounsaturated C24 sphingolipids. Based on our results (Fig. 1*B* and Fig. S6) and others' published reports (Table S1), we propose a model for mammalian VLCFA elongation pathways (Fig. 1*D*). However, precise determination of each pathway will require future biochemical and *in vivo* studies.

**CERS2 regulates C24-CoA synthesis**

Since C24-CoA is almost exclusively used for sphingolipid synthesis, we speculated that some link between sphingolipid synthesis and VLCFA elongation might exist. Therefore, we performed an *in vitro* VLCFA elongase assay in the presence of fumonisin $B_1$ ($FB_1$), a specific inhibitor of Cer synthesis. When C20:0- or C22:0-CoA was used as a substrate, $FB_1$ inhibited the elongation reaction (Fig. 4*A*). However, $FB_1$ had no effect on the elongation of C16:0-, C18:0-, or C18:3(n-3)-CoA.

In HeLa cells, CERS2, 4, and 5 are endogenously expressed (23), so we next determined which CERS was responsible for the $FB_1$-dependent inhibition of elongation, using knock-down analysis with siRNAs specific for *CERS2*, *4*, or *5* (Fig. 4*B*). Neither *CERS4* nor *CERS5* siRNA affected the elongation of any acyl-CoAs tested. However, *CERS2* siRNA specifically inhibited the elongation of C20:0- and C22:0-CoAs (Fig. 4*C*).; this effect was reversed by the introduction of mouse *CerS2* plasmid into the siRNA-treated HeLa cells (Fig. S7). CERS2 is known to be important for C24 Cer synthesis (3, 24). Both of the reactions inhibited by $FB_1$ or *CERS2* siRNA, i.e. the elongations of C20:0- and C22:0-CoAs, are

essential for the production of C24-CoA, the CERS2 substrate. Remarkably, ELOVL1 is responsible for both reactions (Fig. 1*B*). Therefore, we examined the interaction between ELOVL1 and CERS2. FLAG-ELOVL1 and HA-CERS2 were expressed in HEK 293T cells, and cell extracts were subjected to co-immunoprecipitation with anti-FLAG antibodies. Two bands were detected by immunoblot for human CERS2, as previously observed for mouse CerS2 (24), in which the upper band was determined to represent an *N*-glycosylation form. FLAG-ELOVL1 specifically precipitated CERS2 of an unglycosylated form (Fig. 4*D*). It is possible that glycosylation of CERS2 regulates the interaction with ELOVL1. CERS4, which exhibits a substrate specificity similar to that of CERS2, did not interact with ELOVL1 (Fig. 4*D*).

In yeast, enzymes involved in the VLCFA elongation cycle form an elongase complex (20). Similarly, in lysates of mammalian cells we observed the co-immunoprecipitation of ELOVL1 with HACD proteins, the enzymes responsible for the third reactions in the VLCFA elongation cycle (25). To investigate whether ELOVL1 also interacts with other components of the VLCFA elongation machinery other than HACD proteins, we performed co-immunoprecipitation experiments using HA-tagged ELOVL1 and FLAG-tagged KAR and TER, the enzymes catalyzing the second and fourth reactions in the VLCFA elongation cycle, respectively. We found that both FLAG-KAR and FLAG-TER were co-immunoprecipitated with HA-ELOVL1 (Fig. S8*A*), suggesting that mammals also form VLCFA elongase complex(es).

We next examined whether CERS2 forms a complex with KAR, TER, or other ELOVLs by co-immunoprecipitation experiments using HA-tagged CERS2 and FLAG-tagged KAR, TER, or ELOVLs. We found that HA-CERS2 precipitated with both KAR and TER, as well as with each of the seven ELOVLs (Fig. S8*B*). This suggests that CERS2 may interact with ELOVL1 not directly but indirectly via common factor(s) in the elongase complex(es), such as

KER, TER, or unidentified subunits.

**C24 sphingolipids are important for membrane microdomain functions**

Sphingolipids and cholesterols form membrane microdomains, and an importance of C24 sphingolipids in microdomain functions has been suggested. Iwabuchi *et al.* found that C24 lactosylceramides are involved in the activation of LYN associated with membrane microdomains, by comparing cells having a high versus a low C24 lactosylceramide content and by loading exogenous C24 lactosylceramides into the cells having low C24 lactosylceramide content (26). With those results in mind, we tested whether a reduction in endogenous C24 sphingolipids by *ELOVL1* siRNA would affect the activation of LYN. HeLa cells expressing LYN-3xFLAG were treated with *ELOVL1* siRNA, and phosphorylated LYN, i.e. its activated form, was examined. Phosphorylated LYN was reduced to 29% in the *ELOVL1* siRNA-treated cells, compared to controls (Fig. 5). A similar effect was observed using siRNA specific for *CERS2* (Fig. 5). Thus, the importance of C24 sphingolipids in the membrane microdomain functions was confirmed.

**Discussion**

Mammals have seven proteins, ELOVL1-7, that share sequence similarities to yeast VLCFA elongases. Synthesis of VLCFAs occurs by cycling through a four-step process, and the first, an elongation step, utilizes such elongases and is rate-limiting. There had been increasing evidence that each ELOVL exhibits characteristic substrate specificity (Table S1). However, an overall understanding of ELOVLs and the elongation pathway had not yet been recognized. In the study presented here, we performed comprehensive biochemical analyses using all ELOVLs and 11 different acyl-CoA substrates. Based on our results and others' published reports (Table S1), we herein update current and accepted knowledge regarding the FA elongation pathways in mammals (Fig. 1*D*).

In *in vitro* studies ELOVL1 exhibited activities toward all of the saturated C18- to C26-CoAs as substrates, with the highest activity toward C22:0-CoA (Fig. 1*B*). Importantly, other ELOVLs, except ELOVL3, could not elongate C20:0- or C22:0-CoA. Since ELOVL3 is expressed only in limited tissues, such as testis, hair follicles, sebaceous glands, and brown adipose tissue in mice exposed to cold stress (Fig. 2) (27, 28), ELOVL1 may be the sole elongase responsible for the production of C22:0-CoA and C24:0-CoA in most tissues. In mammals, C24:0-CoA and C24:1-CoA are mainly used for C24 sphingolipid synthesis, and ELOVL1 has an important role in its synthesis, as determined here by knock-down analysis (Fig. 3*C* and *D*). Sphingolipids with VLCFAs provide several important functions in mammalian physiology. For example, the C24 lactosylceramides found in microdomains are important for activation of LYN and cell signaling in neutrophils (26). It is notable, then that knock-down of the *ELOVL1* mRNA caused a reduction in the activity of LYN (Fig. 5). A recent report analyzing *CerS2* knockout mice revealed that a deficiency in C24 sphingolipid synthesis results in myelin sheath defects, cerebellar degeneration, and hepatopathy (3, 14). Moreover, the VLCFA moiety of sphingolipids may be important for determination in

molecular species of sphingolipids, since C24 FAs are used in the gangliosides GM3 and GD3 but not in other gangliosides with more complex sugar structures (29). In further support of this, we recently revealed that VLCFA synthesis in yeast is important for the efficient production of complex sphingolipids (30).

Although membrane fractions overproducing ELOVL1 exhibited weak activity toward C18:0-CoA *in vitro* (Fig. 1*B*), knock-down of *ELOVL1* in HeLa cells resulted in greatly reduced (to ~40%) elongase activity toward C18:0-CoA (Fig. 3*A*) and in an accumulation of C18:0 SM (Fig. 3*D*). These results indicate that ELOVL1 is a major C18:0 elongase, at least in HeLa cells grown under our experimental conditions. It is possible that ELOVL1 is expressed more predominantly than other C18:0 elongases in HeLa cells. Alternatively, perhaps overproduced ELOVL1 could not exert full activity in our assay conditions due to insufficient amounts of its regulatory components such as CERS2. We determined that elongation of C20:0- and C22:0-CoAs is regulated by CERS2 (Fig. 4*C*). Both elongations are essential steps for C24 Cer synthesis and are catalyzed by ELOVL1. Although the molecular mechanism of the regulation of ELOVL1 by CERS2 remains unclear, we speculate that CERS2 facilitates the release of the product generated by the ELOVL1 elongase complex, C24-CoA. Without the aid of CERS2, C24-CoA may be stuck within the elongase complex, leading to an inhibition of the next reaction round. Association of CERS2 with the elongase complex (Fig. 4*D* and Fig. S8*B*) may enable CERS2 to efficiently transfer C24-CoAs from the elongase complex to the catalytic site of CERS2, where a C24-CoA and a long-chain base react to produce C24 Cer. We hypothesize that this mechanism may ensure that the production of C24-CoA by elongation is coordinated with its utilization. Consistent with our results, a recent report demonstrated that the levels of C24-CoAs were nearly unchanged in *CerS2* knockout mice, while the other CerS2 substrate dihydrosphingosine accumulated (13).

Our results update and enhance the overall picture of the VLCFA elongation cycles.

Specific inhibitors for certain ELOVLs may be useful in studying or even treating several pathologies in which VLCFAs are involved; knowing the preferred substrates may aid the creation of such inhibitors. In an early example of such a feat, *Elovl6* knockout mice were found to exhibit marked protection from hyperinsulinemia, hyperglycemia, and hyperleptinemia (31). Based on this finding, a specific inhibitor for ELOVL6 was designed for utility as a pharmacological tool (32). Moreover, if certain drugs can induce a metabolic shift from LCFAs to VLCFAs, several metabolic disorder syndromes involving LCFAs may be improved. Future studies are required to elucidate the molecular mechanisms of the regulation and functions of specific ELOVL under certain pathologies.

## Materials and methods

Detailed materials and methods used for all procedures are available in *SI Text*.

## *In vitro* FA elongation assays

*In vitro* FA elongation assays were performed essentially as described elsewhere (15) using total membrane fractions. Typical reaction mixtures of FA elongation assays contained total membrane fractions (20 μg protein), 50 μM acyl-CoA complexed with 0.2 mg/ml FA-free bovine serum albumin (Sigma), and 0.075 μCi [$^{14}$C]malonyl-CoA (55 mCi/mmol; Moravek Biochemicals, Brea, CA) in a 50 μl reaction mixture. When FAs were used in place of acyl-CoAs, reaction mixtures contained total membrane fractions (40 μg protein), 50 μM FAs, 200 μM CoA, 10 mM ATP, and 0.075 μCi [$^{14}$C]malonyl-CoA.

## Lipid analysis by LC/MS

The amounts of SMs were determined by LC/electron spray ionization(ESI)-MS/MS essentially as described elsewhere (33, 34). Lipids were resolved by HPLC (Agilent 1100 series; Agilent Technologies, Palo Alto, CA) on a normal-phase column (Inertsil SIL100A 3 μm, 2.1 x 100 mm; GL Science, Tokyo, Japan). The ESI-MS/MS analyses were performed using an ion trap mass spectrometer LCQ Fleet (Thermo Fisher Scientific Inc, Waltham, MA). The data were analyzed and quantified using the XCalibur software (Thermo Fisher Scientific Inc).

## RNA interference

The control siRNA and siRNAs for *CERS2*, *CERS4*, and *CERS5* were purchased from Qiagen (Hilden, Germany) and have been described previously (23). The nucleotide sequences of *ELOVL1* siRNA were 5’-CCUGUACUACGGAUUAUCUGC-3’ (sense) and

5’-AGAUAAUCCGUAGUACAGGUA-3’ (antisense), and the corresponding duplex siRNA was purchased from Sigma.

**References**


1. Hodson L, Skeaff CM, Fielding BA (2008) Fatty acid composition of adipose tissue and blood in humans and its use as a biomarker of dietary intake. *Prog Lipid Res* 47:348-380.
2. Mizutani Y, Mitsutake S, Tsuji K, Kihara A, Igarashi Y (2009) Ceramide biosynthesis in keratinocyte and its role in skin function. *Biochimie* 91:784-790.
3. Imgrund S, et al. (2009) Adult ceramide synthase 2 (CerS2) deficient mice exhibit myelin sheath defects, cerebellar degeneration and hepatocarcinomas. *J Biol Chem* 284:33549-33560.
4. Buczynski MW, Dumlao DS, Dennis EA (2009) An integrated omics analysis of eicosanoid biology. *J Lipid Res* 50:1015-1038.
5. Torrejon C, Jung UJ, Deckelbaum RJ (2007) n-3 Fatty acids and cardiovascular disease: actions and molecular mechanisms. *Prostaglandins Leukot Essent Fatty Acids* 77:319-326.
6. Sonnino S, et al. (2009) Role of very long fatty acid-containing glycosphingolipids in membrane organization and cell signaling: the model of lactosylceramide in neutrophils. *Glycoconj J* 26:615-621.
7. Soupene E, Kuypers FA (2008) Mammalian long-chain acyl-CoA synthetases. *Exp Biol Med* 233:507-521.
8. Leonard AE, Pereira SL, Sprecher H, Huang YS (2004) Elongation of long-chain fatty acids. *Prog Lipid Res* 43:36-54.
9. Jakobsson A, Westerberg R, Jacobsson A (2006) Fatty acid elongases in mammals: their regulation and roles in metabolism. *Prog Lipid Res* 45:237-249.
10. Revardel E, Bonneau M, Durrens P, Aigle M (1995) Characterization of a new gene family developing pleiotropic phenotypes upon mutation in Saccharomyces cerevisiae.

*Biochim Biophys Acta* 1263:261-265.

11. Tvrdik P, et al. (1997) Cig30, a mouse member of a novel membrane protein gene family, is involved in the recruitment of brown adipose tissue. *J Biol Chem* 272:31738-31746.
12. Ejsing CS, et al. (2009) Global analysis of the yeast lipidome by quantitative shotgun mass spectrometry. *Proc Natl Acad Sci USA* 106:2136-2141.
13. Pewzner-Jung Y, et al. (2010) A critical role for ceramide synthase 2 in liver homeostasis: I. Alterations in lipid metabolic pathways. *J Biol Chem* 285:10902-10910.
14. Pewzner-Jung Y, et al. (2010) A critical role for ceramide synthase 2 in liver homeostasis: II. insights into molecular changes leading to hepatopathy. *J Biol Chem* 285:10911-10923.
15. Moon YA, Shah NA, Mohapatra S, Warrington JA, Horton JD (2001) Identification of a mammalian long chain fatty acyl elongase regulated by sterol regulatory element-binding proteins. *J Biol Chem* 276:45358-45366.
16. Leonard AE, et al. (2002) Identification and expression of mammalian long-chain PUFA elongation enzymes. *Lipids* 37:733-740.
17. Leonard AE, et al. (2000) Cloning of a human cDNA encoding a novel enzyme involved in the elongation of long-chain polyunsaturated fatty acids. *Biochem J* 350 Pt 3:765-770.
18. Inagaki K, et al. (2002) Identification and expression of a rat fatty acid elongase involved in the biosynthesis of C18 fatty acids. *Biosci Biotechnol Biochem* 66:613-621.
19. Oh CS, Toke DA, Mandala S, Martin CE (1997) *ELO2* and *ELO3*, homologues of the *Saccharomyces cerevisiae ELO1* gene, function in fatty acid elongation and are required for sphingolipid formation. *J Biol Chem* 272:17376-17384.
20. Denic V, Weissman JS (2007) A molecular caliper mechanism for determining very

long-chain fatty acid length. *Cell* 130:663-677.

21. Silve S, et al. (1996) The immunosuppressant SR 31747 blocks cell proliferation by inhibiting a steroid isomerase in Saccharomyces cerevisiae. *Mol Cell Biol* 16:2719-2727.

22. Tvrdik P, et al. (2000) Role of a new mammalian gene family in the biosynthesis of very long chain fatty acids and sphingolipids. *J Cell Biol* 149:707-718.

23. Mizutani Y, Kihara A, Chiba H, Tojo H, Igarashi Y (2008) 2-Hydroxy-ceramide synthesis by ceramide synthase family: enzymatic basis for the preference of FA chain length. *J Lipid Res* 49:2356-2364.

24. Mizutani Y, Kihara A, Igarashi Y (2005) Mammalian Lass6 and its related family members regulate synthesis of specific ceramides. *Biochem J* 390:263-271.

25. Ikeda M, et al. (2008) Characterization of four mammalian 3-hydroxyacyl-CoA dehydratases involved in very long-chain fatty acid synthesis. *FEBS Lett* 582:2435-2440.

26. Iwabuchi K, et al. (2008) Involvement of very long fatty acid-containing lactosylceramide in lactosylceramide-mediated superoxide generation and migration in neutrophils. *Glycoconj J* 25:357-374.

27. Westerberg R, et al. (2004) Role for ELOVL3 and fatty acid chain length in development of hair and skin function. *J Biol Chem* 279:5621-5629.

28. Westerberg R, et al. (2006) ELOVL3 is an important component for early onset of lipid recruitment in brown adipose tissue. *J Biol Chem* 281:4958-4968.

29. Ando S, Yu RK (1984) Fatty acid and long-chain base composition of gangliosides isolated from adult human brain. *J Neurosci Res* 12:205-211.

30. Kihara A, Sakuraba H, Ikeda M, Denpoh A, Igarashi Y (2008) Membrane topology and essential amino acid residues of Phs1, a 3-hydroxyacyl-CoA dehydratase involved in

very long-chain fatty acid elongation. *J Biol Chem* 283:11199-11209.

31. Matsuzaka T, et al. (2007) Crucial role of a long-chain fatty acid elongase, Elovl6, in obesity-induced insulin resistance. *Nat Med* 13:1193-1202.

32. Shimamura K, et al. (2009) 5,5-Dimethyl-3-(5-methyl-3-oxo-2-phenyl-2,3-dihydro-1H-pyrazol-4-yl)-1-phe nyl-3-(trifluoromethyl)-3,5,6,7-tetrahydro-1H-indole-2,4-dione, a potent inhibitor for mammalian elongase of long-chain fatty acids family 6: examination of its potential utility as a pharmacological tool. *J Pharmacol Exp Ther* 330:249-256.

33. Houjou T, Yamatani K, Imagawa M, Shimizu T, Taguchi R (2005) A shotgun tandem mass spectrometric analysis of phospholipids with normal-phase and/or reverse-phase liquid chromatography/electrospray ionization mass spectrometry. *Rapid Commun Mass Spectrom* 19:654-666.

34. Merrill AH, Jr., Sullards MC, Allegood JC, Kelly S, Wang E (2005) Sphingolipidomics: high-throughput, structure-specific, and quantitative analysis of sphingolipids by liquid chromatography tandem mass spectrometry. *Methods* 36:207-224.

**Acknowledgments**

We are grateful to Dr. E. A. Sweeney for scientific editing of the manuscript and to Seiko Oka (Hokkaido University) for assistance with the GC/MS. This work was supported by a Grant-in-Aid for Young Scientists (A) (20687008) from the Ministry of Education, Culture, Sports, Sciences and Technology of Japan and in part by grants from the Naito Foundation and from the ONO Medical Research Foundation.

**Figure legends**

Fig. 1. Each ELOVL protein exhibits a characteristic substrate specificity. HEK 293T cells were transfected with a vector (pCE-puro 3xFLAG-1) or a plasmid encoding the indicated 3xFLAG-tagged human ELOVL protein. (*A*) Total membrane proteins (0.1 μg protein) prepared from the transfected cells were treated with Endo H, separated by SDS-PAGE, and detected by immunoblotting with anti-FLAG antibodies. (*B*) Total membrane proteins (20 μg protein) were incubated with the indicated acyl-CoA (50 μM) and 0.075 μCi [$^{14}$C]malonyl-CoA for 30 min at 37°C. After termination of the reactions, lipids were saponified, acidified, extracted, and separated by normal-phase TLC, followed by detection and quantification by a bioimaging analyzer BAS-2500. Values presented are FA levels and represent the mean ± S.D. from three independent experiments. Statistically significant differences compared to vector transfected cells are indicated (*$p<0.05$, **$p<0.01$; t-test) (*C*) Total membrane proteins (20 μg protein) were incubated with C18:0- or C20:0-CoA (20 μM) and 100 μM (0.075 μCi) [$^{14}$C]malonyl-CoA for 30 min at 37°C. After termination of the reactions, lipids were subjected to methanolysis, extraction, separation by reverse-phase TLC, and detection by BAS-2500. (*D*) VLCFA elongation pathways found in mammals and the ELOVLs proposed to be involved in each pathway are illustrated. The numbers located on the left side of the arrows indicate the ELOVL protein (ELOVL1-7). Parenthesis exhibits weak activities of those enzymes in the indicated reactions. SFA, saturated FA; MUFA, monounsaturated FA.

Fig. 2. Tissue-specific expression patterns of human *ELOVL* mRNAs. *ELOVL* and *GAPDH* cDNAs were amplified by PCR from human tissue cDNAs or from the pCE-puro 3xFLAG-ELOVLx plasmid using specific primers. Amplified fragments were separated by agarose gel electrophoresis and stained with ethidium bromide.

Fig. 3. ELOVL1 is important for C24 sphingolipid production. HeLa cells were transfected with 16 nM control or *ELOVL1* siRNA 4 days prior to experiments. (*A*) Total membrane proteins (40 μg) were incubated with the indicated acyl-CoA (50 μM) and 0.025 μCi [$^{14}$C]malonyl-CoA for 1 h at 37°C. After termination of the reactions, lipids were saponified, acidified, extracted, and separated by TLC, followed by detection and quantification by a bioimaging analyzer BAS-2500. Values represent the mean ± S.D. from three independent experiments. Statistically significant differences are indicated (**p<0.01; t-test). (*B*) Total RNA was prepared from the transfected cells and subjected to RT-PCR using primers specific for *ELOVL1* or *GAPDH*. (*C*) Cells were labeled with 2 μCi [$^{3}$H]sphingosine for 2 h at 37°C. Lipids were extracted, separated by reverse-phase TLC, and detected by autoradiography (right panel). The left panel shows C16:0 Cer, C20:0 Cer, C24:0 Cer, and C24:1 Cer standards, each at 10 nmol, separated by reverse-phase TLC and stained with cupric acetate/phosphoric acid solution. (*D*) Lipids were extracted from the transfected cells and subjected to LC/ESI-MS/MS analysis. SM ions, determined as those losing the 60 Da neutral ion, were quantified. Values represent the relative amounts of certain SM species compared to total SM levels, and are the mean ± S.D. from three independent experiments. Note that ionization efficiencies varied among molecular species of SMs. Statistically significant differences are indicated (**p<0.01; t-test). E1, ELOVL1; cont., control.

Fig. 4. CERS2 regulates ELOVL1 activity. (*A*) Total membrane proteins (40 μg) prepared from HEK 293T cells were incubated with the indicated acyl-CoA (40 μM) and 0.025 μCi [$^{14}$C]malonyl-CoA in the presence or absence of 20 μM $FB_1$ for 1 h at 37 ˚C. After termination of the reactions, lipids were saponified, acidified, extracted, and separated by TLC, followed by detection and quantification by a bioimaging analyzer BAS-2500. Values represent the

mean ± S.D. from three independent experiments. Statistically significant differences are indicated (*p<0.05, **p<0.01; t-test). (*B*) HeLa cells were transfected with the indicated siRNAs (6 nM) 4 days prior to experiments. Total RNA was prepared then subjected to RT-PCR using primers specific for *CERS2*, *CERS4*, *CERS5* or *GAPDH*. (*C*) Total membrane proteins (40 μg) prepared from HeLa cells transfected with the indicated siRNAs were subjected to an *in vitro* elongase assay as in (*A*) using the indicated acyl-CoA (50 μM) and 0.04 μCi [$^{14}$C]malonyl-CoA. Values represent the mean ± S.D. from three independent experiments. Statistically significant differences are indicated (*p<0.05; t-test). (*D*) HEK 293T cells were transfected with a pcDNA3 HA-1 control vector, or a pcDNA3 HA-CERS2 or pcDNA3 HA-CERS4 plasmid, and with a pCE-puro 3xFLAG-ELOVL1 plasmid or pCE-puro 3xFLAG-1 control vector. Total cell lysates were prepared from the transfected cells and solubilized with 1% Triton X-100. Total lysates (left panel) or proteins immunoprecipitated with anti-FLAG M2 agarose (right panel) were subjected to immunoblotting with anti-FLAG or anti-HA antibodies. IP, immunoprecipitation; IB, immunoblotting; Total, total cell lysates.

Fig. 5. Knock-down of *ELOVL1* mRNA causes a reduction in LYN activity. HeLa cells were transfected with control, *ELOVL1*, *ELOVL3*, *CERS2*, or *CERS4* siRNAs (15 nM) 4 days prior to experiments, and with the pCE-puro LYN-3xFLAG plasmid 2 days prior to experiments. Total lysates were prepared from the cells, solubilized with Triton X-100, and immunoprecipitated with anti-FLAG M2 antibodies. Immunoprecipitates were incubated with 5 μCi [γ-$^{32}$P]ATP for 5 min at 37°C, then separated by SDS-PAGE and detected by autoradiography (upper panel) or by immunoblotting with anti-FLAG antibodies (lower panel). p-LYN, phosphorylated LYN.

Figure 1

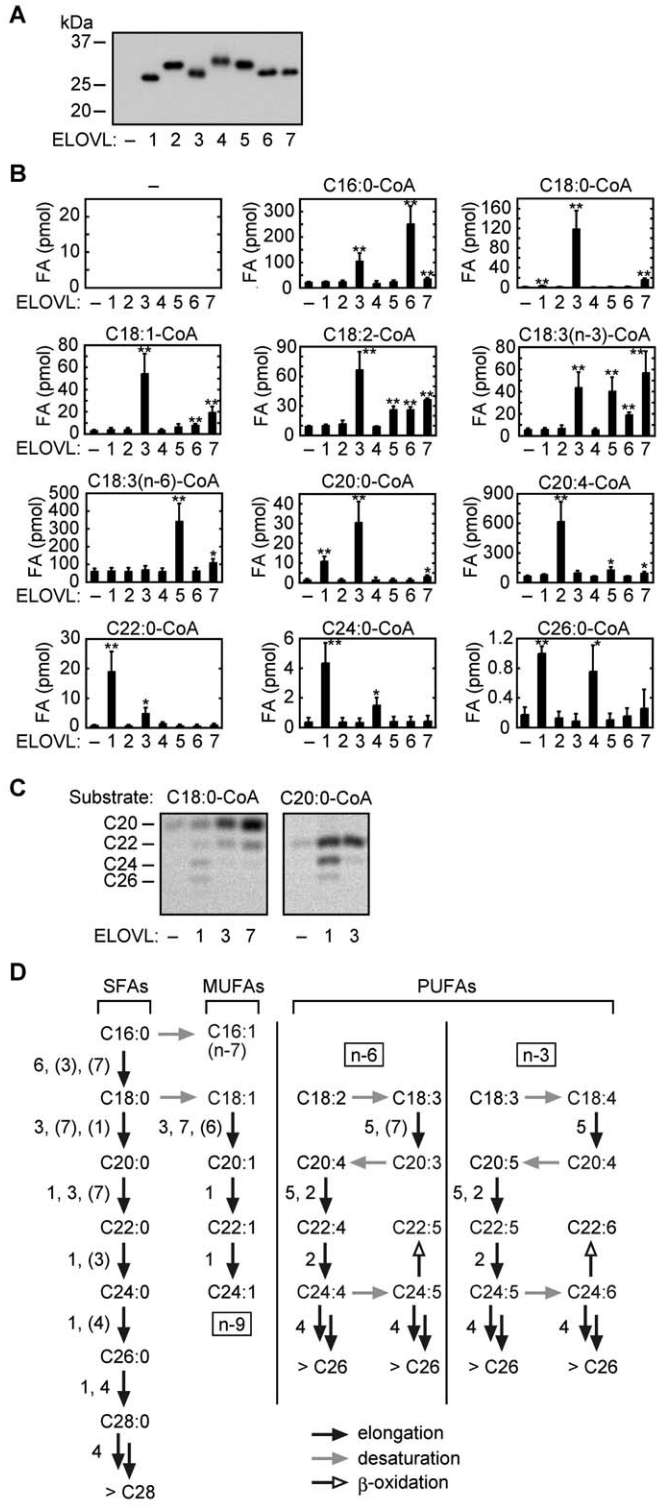
A
kDa
37
25
20
ELOVL: – 1 2 3 4 5 6 7
B
–
C16:0-CoA
C18:0-CoA
C18:1-CoA
C18:2-CoA
C18:3(n-3)-CoA
C18:3(n-6)-CoA
C20:0-CoA
C20:4-CoA
C22:0-CoA
C24:0-CoA
C26:0-CoA
FA (pmol)
ELOVL: – 1 2 3 4 5 6 7
C
Substrate: C18:0-CoA C20:0-CoA
C20
C22
C24
C26
ELOVL: – 1 3 7 – 1 3
D
SFAs
MUFAs
PUFAs
C16:0
C16:1 (n-7)
6, (3), (7)
C18:0
C18:1
3, (7), (1)
3, 7, (6)
C20:0
C20:1
1, 3, (7)
1
C22:0
C22:1
1, (3)
1
C24:0
C24:1
1, (4)
n-9
C26:0
1, 4
C28:0
4
> C28
n-6
C18:2
C18:3
5, (7)
C20:4
C20:3
5, 2
C22:4
C22:5
2
C24:4
C24:5
4
4
> C26
> C26
n-3
C18:3
C18:4
5
C20:5
C20:4
5, 2
C22:5
C22:6
2
C24:5
C24:6
4
4
> C26
> C26
elongation
desaturation
β-oxidation

Figure 2

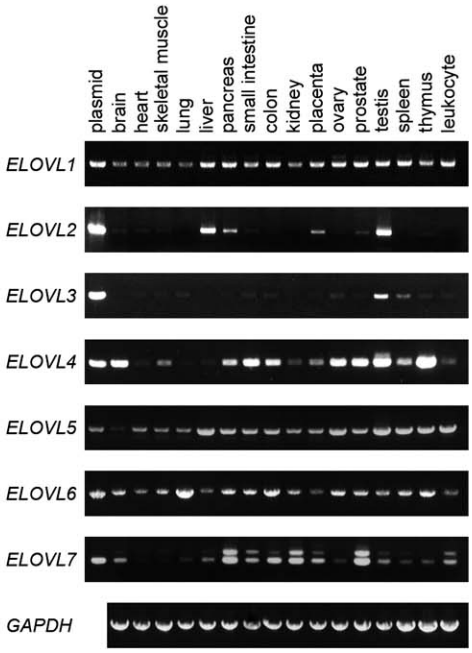
plasmid
brain
heart
skeletal muscle
lung
liver
pancreas
small intestine
colon
kidney
placenta
ovary
prostate
testis
spleen
thymus
leukocyte
ELOVL1
ELOVL2
ELOVL3
ELOVL4
ELOVL5
ELOVL6
ELOVL7
GAPDH

Figure 3

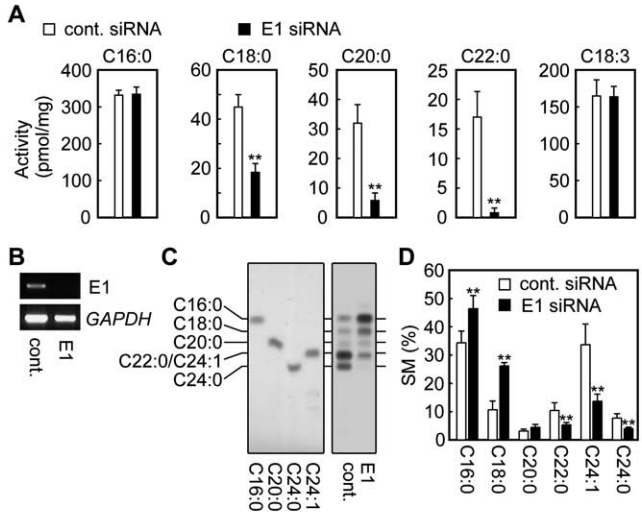
A
cont. siRNA
E1 siRNA
C16:0
C18:0
C20:0
C22:0
C18:3
Activity (pmol/mg)
B
E1
GAPDH
cont.
E1
C
C16:0
C18:0
C20:0
C22:0/C24:1
C24:0
C16:0
C20:0
C24:0
C24:1
E1
cont.
D
cont. siRNA
E1 siRNA
SM (%)
C16:0
C18:0
C20:0
C22:0
C24:1
C24:0

# Figure 4

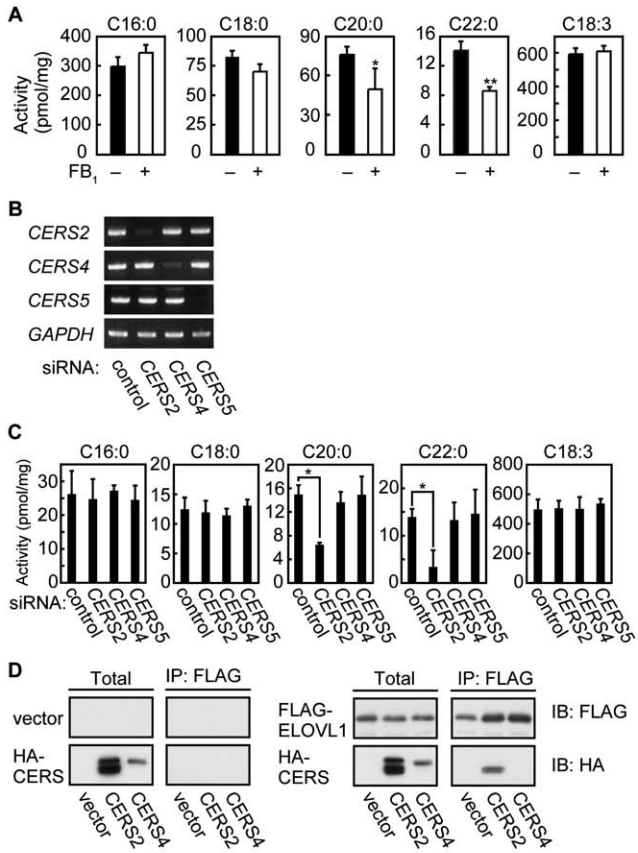
A
C16:0
C18:0
C20:0
C22:0
C18:3
Activity (pmol/mg)
FB1 – +
B
CERS2
CERS4
CERS5
GAPDH
siRNA: control CERS2 CERS4 CERS5
C
Activity (pmol/mg)
siRNA: control CERS2 CERS4 CERS5
D
Total
IP: FLAG
vector
HA-CERS
FLAG-ELOVL1
IB: FLAG
IB: HA
vector CERS2 CERS4

Figure 5

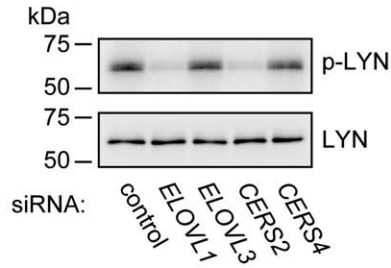
kDa
75
50
75
50
p-LYN
LYN
siRNA:
control
ELOVL1
ELOVL3
CERS2
CERS4